The age of evapotranspiration: continental-scale lower-bound constraints from distributed water fluxes

W.J. Hahm[1], D.A. Lapides[1,2], D.M. Rempe[3], E.L. McCormick[3], D.N. Dralle[2]

[1]Simon Fraser University, Burnaby, BC, Canada

[2]Pacific Southwest Research Station, United States Forest Service, Davis, CA, USA

[3]University of Texas at Austin, Austin, TX, USA

Key Points:

- A last-in, first-out (LIFO) selection of stored water for evapotranspiration yields the minimum flux-weighted age
- A LIFO-based continental-scale evapotranspiration minimum age map was created via cloud computation with distributed water flux timeseries
- The minimum flux-weighted evapotranspiration age is greatest in the Western US in seasonally dry and (semi-)arid biomes

Corresponding author: W.J. Hahm, `whahm@sfu.ca`

Abstract

Unlike streamflow, which can be sampled in aggregate at the catchment outlet, evapotranspiration (ET) is spatially dispersed, challenging large-scale age estimation. Here, we introduce an approach for constraining the age of ET via mass balance and present the minimum flux-weighted age of ET across the continental US using distributed, publicly available water flux datasets. The lower-bound constraint on ET age can be calculated by assuming that ET is preferentially sourced from the most recent precipitation through a last-in, first-out algorithm. From 2012-2017, ET was at least several months old across large areas of the western continental US, including in Mediterranean and (semi-)arid climate zones and shrub and evergreen needleleaf plant communities. The primary limitation of this approach is that it provides only a minimum flux-weighted average age to satisfy mass balance of outgoing fluxes; true ET fluxes are composed of distributions of ages and may be composed of much older water. The primary advantage of the approach is that flux timeseries of precipitation and ET are sufficient to constrain ET age, and model parameterization is unnecessary. ET ages can be used to validate tracer-aided and modeling approaches and inform studies of biogeochemistry, water-rock interactions, and plant water sourcing under drought.

Plain Language Summary

What is the age of water returned to the atmosphere from the terrestrial land surface? Here, we explore the results of a simple mass-balance approach that yields the minimum age of evapotranspired water by assuming that evapotranspiration sources water from the most recently arrived precipitation available. Newly arriving precipitation is added to an age ranked storage reservoir, and the youngest water in the storage reservoir is withdrawn for evapotranspiration. We demonstrate that this last-in, first-out selection of water from storage for evapotranspiration results in a lower bound average age over a time period of record, even without knowledge of other outgoing fluxes like stream discharge. Cloud computation enables the creation of a minimum flux-weighted ET age map across the continental US from distributed, publicly available precipitation and evapotranspiration datasets. The results of this study constrain an otherwise challenging property of the hydrologic cycle to monitor, as the lack of tracer data (e.g. water isotope concentrations) in evapotranspiration at the continental scale makes quantifying age with traditional transit time approaches infeasible without significant model parameter assumptions.

1 Introduction

The age of evapotranspired water can be defined as the elapsed time between when precipitation falls and when that water returns to the atmosphere as vapor via transpiration or abiotic evaporation (Botter et al., 2011). Thus, the age of ET describes the transit time distribution of water molecules through terrestrial storage (including above-ground such as snow or lakes, subsurface, and intra-plant storage) before being incorporated into the primary outflow of the terrestrial hydrologic cycle (Schlesinger & Jasechko, 2014). The age of ET can provide information about the origins of plant water sources (Miguez-Macho & Fan, 2021), the sensitivity of those sources to drought (Rempe et al., pre-print), and nutrient supply, which depends on water residence time in reactive belowground environments (Li et al., 2017). For example, fluid residence time in belowground environments is a primary determinant of chemical weathering rates (Maher, 2010) and therefore the dissolution of rock-derived plant-essential elements like phosphorous and potassium. The age of water used by plants may therefore constrain the uptake of those nutrients.

Although major advances have been achieved in quantifying the time-varying transit times of stream discharge (the other dominant outgoing flux in the land-component of the hydrologic cycle; Rinaldo et al., 2015; McGuire & McDonnell, 2006), our understanding of the age of ET is comparatively limited (Soulsby et al., 2016; Sprenger et al., 2019). This is due in large part to challenges in measuring tracers in ET: unlike streamflow, which is an aggregated flux that can be readily sampled to parameterize age models (e.g. Lapides et al., 2022), ET is a dispersed flux, making sampling logistically challenging at large spatiotemporal scales (e.g. Allen et al., 2019). Furthermore, tracer-aided ecohydrologic model-based approaches to constraining ET ages (Maxwell et al., 2019; Wilusz et al., 2020; Miguez-Macho & Fan, 2021; Kuppel et al., 2020; Smith et al., 2021) are potentially limited by inaccurate parameterizations of subsurface water storage reservoirs and persistent challenges in uniquely identifying plant water uptake patterns through time. For example, plant water use from bedrock is routine and widespread (McCormick et al., 2021), but this phenomenon is poorly incorporated into most land surface models. Few field-based isotope studies to date have routinely sampled unsaturated bedrock below the soil for water isotopes (e.g. Hahm et al., 2020).

Constraints on reservoir storage properties (including the size of the reservoir and the age of water in storage) may also be obtained from timeseries of fluxes into and out of the reservoir. Such mass balance approaches bypass the need for extensive isotopic sampling campaigns and avoid errors potentially introduced by inaccurate model parameterization, but they generally provide only an upper or lower bound on a reservoir property of interest rather than an exact value. For example, mass balance approaches have been used to infer a minimum subsurface water storage capacity (Wang-Erlandsson et al., 2016; Dralle et al., 2021). These approaches use fluxes of ET and precipitation to determine how much water must be supplied from storage to explain observed ET in excess of precipitation (termed a 'deficit') over a certain time period. A minimum bound on the storage capacity is achieved by the observation that the reservoir must have a capacity that matches or exceeds that largest deficit observed.

Here, we apply an analogous approach for quantifying a lower bound estimate of the age of evapotranspired water. This is achieved by requiring evapotranspiration to source water from the most recently arrived precipitation in storage. This approach yields ET ages that are in general less than true ET ages, but has the advantage of being parameter-free and readily applicable at continental scales using only publicly available distributed water flux datasets. Here, we use this approach to ask: what is the spatial pattern of the flux-weighted minimum ET age across the continental US, and how does it vary with climate and plant community? The result of this exercise provides a new benchmark ET age dataset to compare against other approaches.

2 Methods

2.1 Estimation procedure

To determine the minimum flux-weighted age of evapotranspiration, a 'last-in, first-out' (LIFO) algorithm is implemented at each timestep for each pixel on the landscape:

1. Newly arriving precipitation (with dimensions of length) is added to an age-ranked storage reservoir (as described by Harman, 2015, 2019).
2. The amount of water needed to supply evapotranspiration at the current timestep is then withdrawn from the youngest water available in the storage reservoir. This amount of water and its age distribution is recorded.
3. After the water required to supply ET is removed from the storage reservoir, the remaining water in storage ages by the timestep, and the procedure repeats for the duration of the timeseries.

An estimate of the minimum flux-weighted average water age of ET at each pixel through time is then determined by weighting the ages at each timestep by the magnitude of the ET flux. Technically the algorithm allows for a distribution of ages at each timestep at a location, but in practice this distribution is usually small (a single age) for small timesteps because ET can be sourced from stored precipitation from a single storm event. In the terminology of storage selection functions (Rinaldo et al., 2015), this approach is equivalent to the ET flux drawing water from storage via a Dirac delta selection function located at the youngest edge of the storage distribution. The LIFO algorithm has been studied in the context of queuing and information theory (where it is sometimes referred to as 'last-come, first-serve' or a stack; Kleinrock, 1975; Tripathi et al., 2019), but to our knowledge has not been explicitly applied in the context of ET ages. No other water flux apart from precipitation is assumed to enter the pixel. Knowledge of other outflows is unnecessary for the calculation procedure since the procedure is intended only to calculate a lower bound: the depletion of stored water via other fluxes out of the pixel (e.g., discharge or groundwater flow) can only result in older water (never younger water) being available for ET, thus preserving the validity of the lower-bound ET age constraint.

In queuing theory, LIFO has been shown to result in minimum ages in a variety of different contexts (Costa et al., 2016; Kaul et al., 2012; Bedewy et al., 2019a, 2019b; Xu & Gautam, 2020). However, LIFO only produces a true minimum average ET age when considered as a flux-weighted average over a sufficiently long time period; it is potentially inaccurate on a given timestep. For example, consider a case where instead of following LIFO, there is a timestep on which ET does not use the youngest water available (ET is older than in LIFO). Then that unused younger water could be used for ET on a later day, resulting in younger ET than would have been possible had the LIFO procedure been followed. In this case, it is possible to achieve a younger ET age on one day but only at the expense of older ET on a different day. This forced trade-off due to mass balance means that, ultimately, the mean ET age achieved through any other selection function is either identical to or older than that achieved using LIFO (based on an extended version of the proof presented by Kingman, 1962). An important distinction between many previous applications of LIFO and this study is that not all precipitation gets used for ET (not all tasks in the queue get served). However, LIFO still produces the youngest mean age in this scenario. For a detailed explanation, see Appendix A. Additional limitations and benefits of this approach are explored in the Discussion.

2.2 Data sources and implementation

Only two datasets are required for the ET age estimation procedure: timeseries of precipitation and evapotranspiration. We use the ≈ 4.5 km pixel resolution daily PRISM precipitation dataset (PRISM Climate Group, 2021; Daly et al., 2008) resampled to 8-days, and the ≈ 500 m pixel resolution, 8-day Penman-Monteith-Leuning evapotranspiration V2 dataset (combined vegetation transpiration, soil evaporation, and interception from vegetation canopy bands) (Zhang et al., 2019). A minimum flux-weighted ET age constraint is maintained even in the presence of intra-timestep variations in the delivery of P and ET due to the order of operations in the algorithm presented above.

Analysis is performed on the Google Earth Engine (GEE) cloud computing platform (Gorelick et al., 2017), accessed via the Python application programming interface with Google Colab computational notebooks. A repository with the code and resulting georeferenced data output rasters are linked below. Proof-of-principle code for implementing the procedure at a single point is also provided. We filtered the data to five water years (2012-10-01 to 2017-10-01) that coincided with the growth and gradual decline of CONUS-scale drought conditions (`https://droughtmonitor.unl.edu/DmData/TimeSeries.aspx`). We masked out pixels with agricultural or urban landcover and locations where evapotranspiration exceeded precipitation (due to, e.g., agricultural or groundwater subsidies or inaccurate flux data). We used default nearest neighbor resampling to export the mean age map to $\approx 0.09°$ (10 km at equator) pixel resolution.

2.3 Contextual datasets

To contextualize the inferred ET ages we compiled and computed a number of additional datasets:

2.3.1 Longest dry period

We calculated the longest dry period on record across the continental US using an existing algorithm (Gorelick, 2021), which determines the longest number of days without precipitation at each pixel using the same PRISM precipitation dataset described above (PRISM Climate Group, 2021).

2.3.2 Asynchronicity index

We calculated the information theory-based asynchronicity index between precipitation (P) and potential evapotranspiration (PET) Feng et al. (2019), which captures both the temporal misalignment and differences in relative magnitudes between atmospheric water delivery and demand; a higher value indicates greater mismatch between P and PET monthly magnitudes and phase, such as would be found in winter-wet, summer-dry Mediterranean climates.

Since PRISM does not explicitly provide a PET data product, we used $\approx$ 4 km pixel-scale monthly average Terraclimate P and PET data (Abatzoglou et al., 2018) from the time period 1958-2020. A negligible quantity (0.001 mm) was added to the monthly averages to ensure no division by zero occurred during calculation of the index.

2.3.3 Mean annual precipitation and evapotranspiration

Mean annual precipitation and evapotranspiration were calculated between 2012-10-01 and 2017-10-01 in the Google Earth Engine platform. Precipitation was averaged from daily time period PRISM data (PRISM Climate Group, 2021). Evapotranspiration was averaged from the combined vegetation transpiration, soil evaporation, and interception from vegetation canopy bands provided in the Penman-Monteith-Leuning Evapotranspiration V2 dataset (Zhang et al., 2019).

2.3.4 Land cover and climate type

We accessed the Annual International Geosphere-Biosphere Programme (IGBP) land cover type classification from the MODIS MCD12Q1 V6 data product (Friedl & Sulla-Menashe, 2015) in GEE, using the most recent year. We excluded mean ages in unsuitable analysis locations, which included permanent wetlands, croplands, urban and built-up lands, cropland/natural vegetation mosaics, permanent snow and ice, barren and water bodies. We accessed the Koeppen-Geiger climate type (Peel et al., 2007) from the GEE asset created by McCormick et al. (2021). The climate types were grouped by the first two letters of the classification scheme. Both of these datasets were resampled (via the statistical mode) to match the ET age pixel resolution. To ensure that land area was weighted appropriately, the raster datasets were analyzed in the Conus Albers equal-area projection.

3 Results

3.0.1 Illustrative timeseries at a point

To illustrate how the LIFO selection function interacts with storage, Figure 1a plots timeseries of cumulative precipitation and evapotranspiration (the input data for ET age estimation) at a semi-arid Blue oak savanna site in the Northern California Coast Range

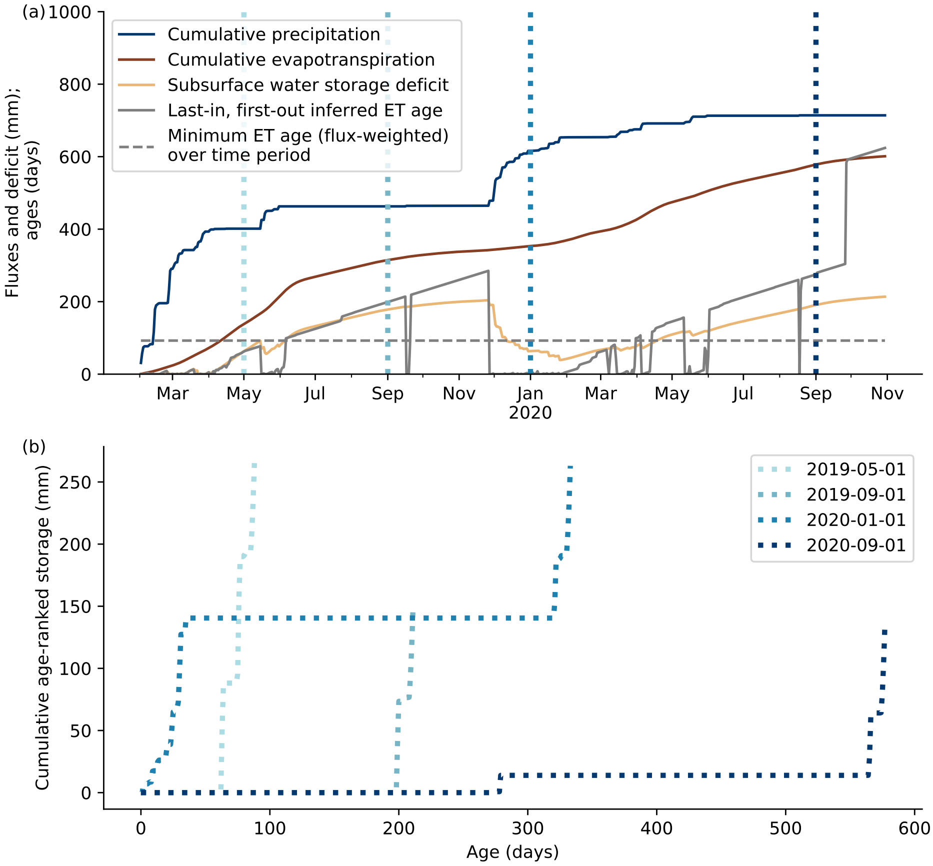

Figure 1. Illustrative timeseries at a single location of (a) input (precipitation) and output (evapotranspiration (ET)) fluxes, storage dynamics, and LIFO-inferred ET age, and (b) age-ranked storage distribution snapshots at four select dates of the water remaining in storage; the dates of the storage snapshots in (b) are shown as vertical dashed lines in (a). The site is a seasonally dry Blue oak savanna in the Northern California Coast Range. See main text for more information on the site.

('Rancho Venada'). The site experiences a rain-dominated Mediterranean climate, with negligible summer precipitation (additional site details are available in Pedrazas et al., 2021; Hahm et al., 2022). A storage deficit (evapotranspiration in excess of precipitation, Wang-Erlandsson et al., 2016) grows through the first dry season and is only partially replenished during the following wet season.

The instantaneous LIFO-inferred average ET age plotted in Figure 1a shows how ET age jumps to zero following rain events, and then increases along a 1:1 aging slope during dry periods as the last precipitation event in storage is used up. Occasional jumps in ET age reflect the complete consumption of the most recent precipitation event, and the need for subsequent ET to be supplied from even older water in storage. A particularly notable age jump occurs in September 2020, when ET has completely consumed the entire precipitation input from that water year, and the next youngest water remaining in storage to supply ET is from the previous water year (there was negligible groundwater recharge and streamflow in the 2021 water year at this site, Hahm et al., 2022). Figure 1a also shows the LIFO-inferred flux-weighted ET age over the plotted time period as a horizontal line, which is the minimum average ET age over this time period.

Figure 1b shows cumulative distributions of age ranked storage at four select times in Figure 1a (where the corresponding times are denoted by matching-color vertical dashed lines). X-axis intercepts mark the age of the youngest water in storage. The two storage snapshots in 2019 follow dry periods. The later 2019 storage snapshot has the same relative age structure as the earlier 2019 snapshot but is translated in this plotting space downward and to the right, due to i) aging of the water in storage (rightward translation) and ii) the net consumption (ET in excess of P) of the youngest water in storage (downward translation) over the time interval. The January 2020 wet season snapshot reveals how during periods with P in excess of ET there is generally ample young water in storage; at this time period the ET age in Figure 1a is close to zero. The final storage snapshot in Figure 1b from September 2020 reveals why a large jump in ET age occurs shortly afterward in Figure 1a. Only about 20 mm of water less than 300 days old (from the current water year) remains in storage at this point in the dry season. Once this water is consumed by ET in the following weeks, the next youngest water available remaining in storage is over 500 days old (delivered as precipitation in the previous water year).

3.0.2 Continental-scale analysis

Figure 2a shows minimum flux-weighted ET ages across the continental US (i.e., this figure maps the value of the horizontal dashed line in Figure 1a for each pixel). Minimum flux-weighted average ET ages are greater than one month across large areas of the western continental US, whereas ET in most of the eastern continental US can be sourced from water less than one month old. In large parts of California and other scattered upland regions, the water supplying ET must be more than three months old on average. Minimum flux-weighted ET ages have a U-shaped relationship to both mean annual precipitation and evapotranspiration (Figure 3), with higher minimum flux-weighted ET ages found at very low and very high P and ET. This pattern varies spatially, however. For example, the northern West Coast, the Sierra Nevada, the Cascade Range, and the central Gulf Coast all have high precipitation, but ET along the central Gulf Coast can be sourced with water younger than one month on average (Figure 2). In general, areas with a higher asynchronicity index are areas with older minimum flux-weighted ET ages (Figure 3). There is also geographic variability in this relationship, with a notable exception in the southeast US, which must have enough summer precipitation to provide young water for ET while still having a relatively large asynchronicity between atmospheric water and energy supply (Figure 2). Areas with long consecutive dry periods also tend to have relatively old minimum flux-weighted ET ages. It may be coincidence that an almost 1:1 slope emerges between minimum flux-weighted age ET and longest

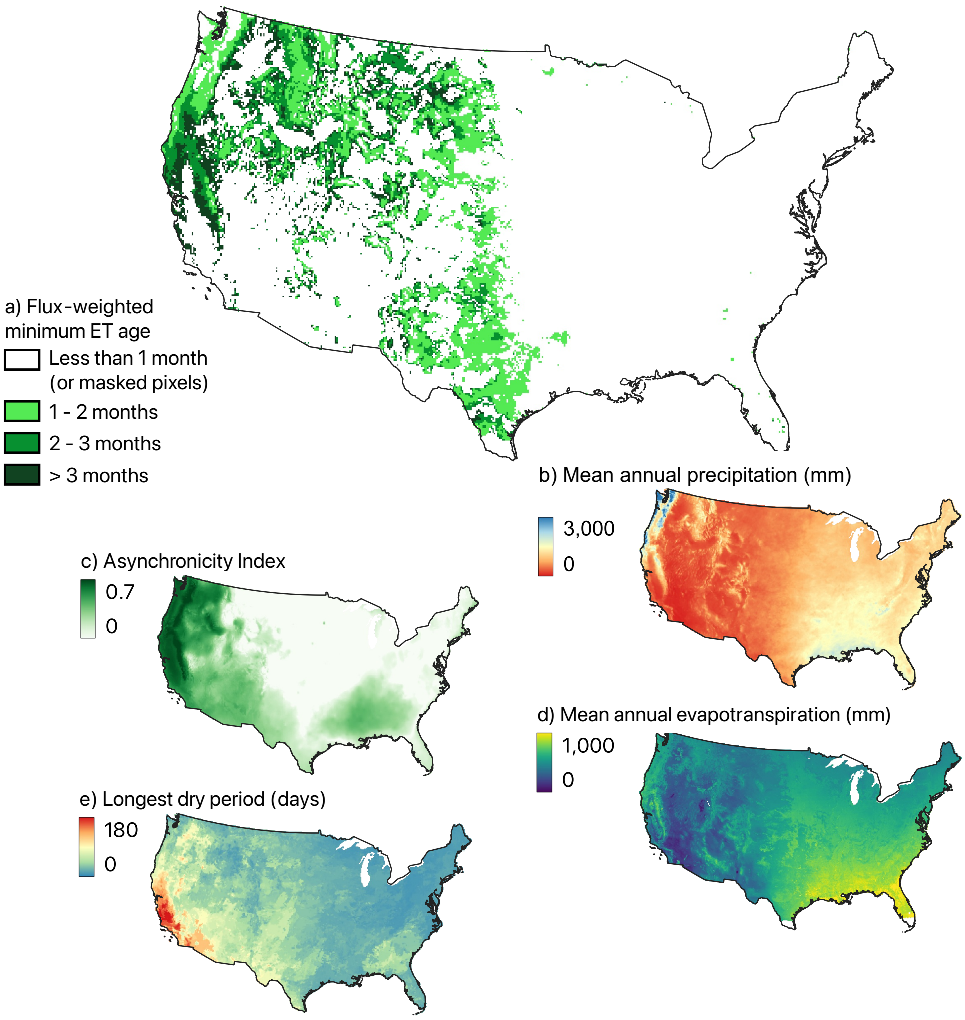

Figure 2. Map of (a) flux-weighted, last-in first-out inferred ET age indicates that ET must be relatively old across much of the western continental US. Maps in (b-e) provide contextual climate metrics for the same area.

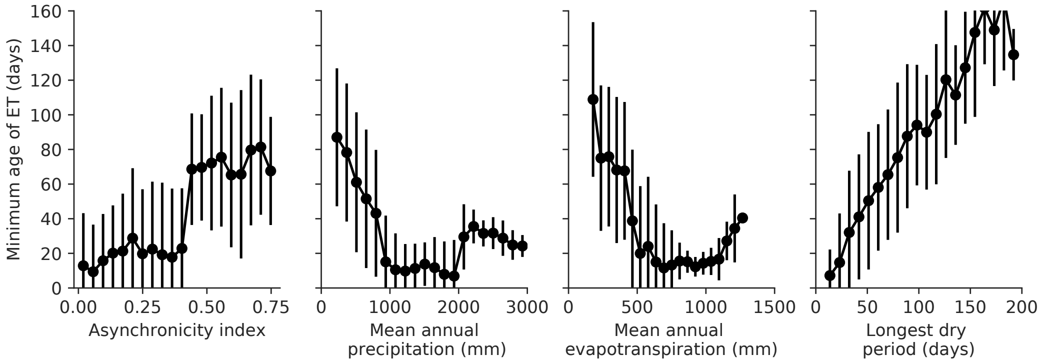

Figure 3. Median values (points) and surrounding one standard deviation ranges (vertical error bars) for lower bound ET ages over the period of record, plotted versus evenly spaced binned values of the contextual dataset maps shown in Figure 2.

dry period (Figure 3), because long dry periods are relatively easy to interrupt (just one day of precipitation restarts the count), whereas replenishing storage with new precipitation to sustain ET is a much longer process.

The boxplots in Figure 4a indicate that relatively old ET comes from desert and arid, Mediterranean, humid continental and subarctic (dry summer), and semi arid climate regions, with more than half of these areas having minimum flux-weighted ET ages greater than two months. In contrast, ET from most non-dry summer humid climate regions may be less than one month old. In terms of plant community type (panel b), shrublands and evergreen needleleaf forests (one of the most productive and highest biomass plant communities in the continental US; Kellndorfer et al., 2013) must have relatively old ET. In contrast, ET from deciduous broadleaf forests (which tend to be concentrated in the eastern continental US) can be sourced from young water (less than one month old).

4 Discussion

4.1 The LIFO ET selection function

The LIFO ET selection function results in a minimum flux-weighted estimation of ET age over a time period of record. Other selection functions that sample the entire distribution of stored water may result in artefactually increasing mean age estimates over time when streamflow out of a pixel is not constrained. This is because in any location where in the long-term P exceeds ET (which is generally the case, in the absence of inter-pixel fluxes), storage grows as time progresses in the absence of streamflow so that the maximum (and likely mean) age of water in storage is positively correlated with the period of record.

Under what conditions is the LIFO-inferred minimum ET age most likely to be similar to the true ET age? One notable case is the scenario in which interception and soil evaporation occur nearly contemporaneously with precipitation, and effectively capture and return incident precipitation to the atmosphere (e.g. Hrachowitz et al., 2013; Crockford & Richardson, 2000). However, the LIFO approach is an obvious underestimation of true age in other scenarios. For example, no distinction is made between rain or snow, and snow must melt before becoming plant available. This may not cause a large divergence between minimum and true ET ages if ET is minimal when snow is present, but some forests transpire through the winter under persistent snowcover (e.g. Kelly & Goulden,

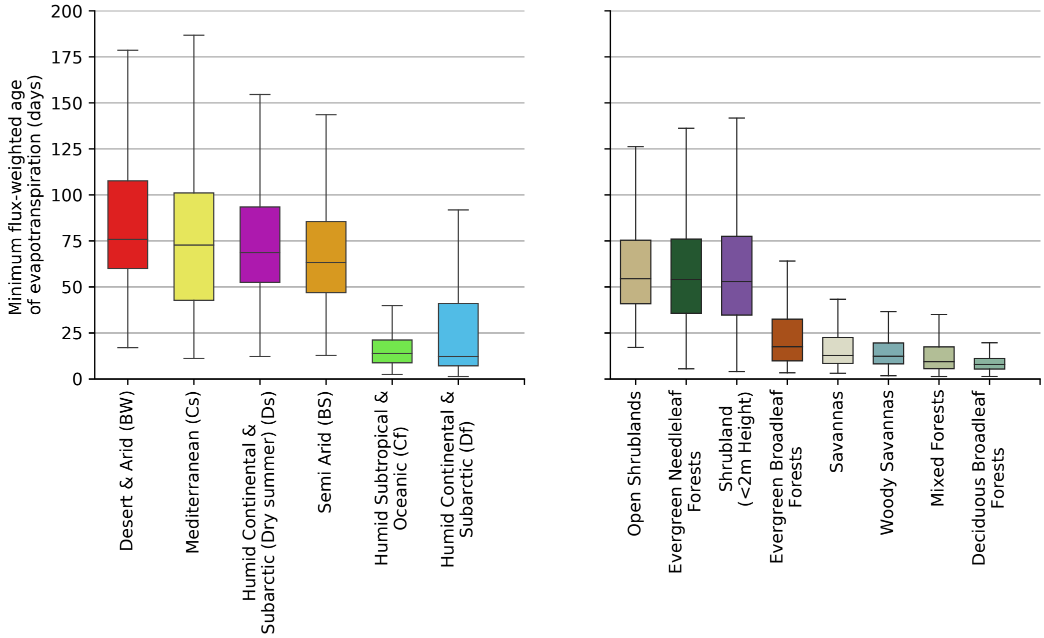

Figure 4. Boxes and whiskers show the quartiles and data bounded within 1.5 times the inter-quartile range beyond the box edges, respectively, of flux-weighted minimum ET age pixels (from Figure 2a) grouped by the most common (by area) Koeppen-Geiger climate types (left) and natural plant communities (right) in the continental US.

2016). LIFO will also underestimate true ET age when stream discharge depletes young water from storage. This can occur, for example, under the following conditions: i) when precipitation falls directly on the channel, ii) when the catchment has wet antecedent conditions (e.g. Harman, 2015), or iii) in catchments that experience infiltration-excess (Hortonian) overland flow. Even if water uptake by plants followed the LIFO selection function, true ET ages will still generally be older than the LIFO inferred age since water must transit plants before transpiring. Intra-plant transit times are likely to be non-negligible particularly for large woody species (e.g. Meinzer et al., 2006; Seeger & Weiler, 2021), with tracer transit times from bole to crown documented on the order of 2.5 to 20 days. Sprenger et al. (2019) estimated a global average mean intra-plant water residence time of 6 days based on storage volumes and fluxes, using data from Oki and Kanae (2006).

4.2 Comparison to other estimations of ET age

Tree-scale studies that have sampled transpiration in experimental laboratory conditions have found contrasting behaviors, with Evaristo et al. (2019) observing relatively older water in the transpiration compared to drainage fluxes (at Biosphere 2), and with Benettin et al. (2021) showing that willow trees took up new tracer water faster than it could drain to the bottom of a lysimeter.

Hillslope- to catchment-scale studies employing a variety of tracers have found that evapotranspiration preferentially selects younger water in storage relative to streamflow (e.g. Soulsby et al., 2016; Visser et al., 2019; Kuppel et al., 2020). Kirchner and Allen (2020) found that most evapotranspiration is sourced from intra-seasonal precipitation at the Hubbard Brook experimental forest in New Hampshire. These findings lend support to the ages inferred by the LIFO selection function. The usual sampling strategy in these studies nevertheless tends to focus on streamwater rather than transpiration, however, and abiotic evaporative fluxes are rarely sampled.

Our simple mass balance approach is broadly consistent with more complicated large-scale models. Using a Lagrangian particle tracking model, Asenjan and Danesh-Yazdi (2020) recently found that plants have a strong preference for the youngest water in storage, and similar to our observations found that the oldest ET ages occurred in locations with pronounced seasonal offsets between P and ET (that is, in locations likely to exhibit a relatively high asynchronicity index). Maxwell et al. (2019) also employed Lagrangian particle tracking within a hydrologic model and found that ET tends to take up younger water in storage.

Miguez-Macho and Fan (2021) recently described a comprehensive, large-scale effort to model the age of water taken up by ET. They concluded that globally more than 70% of plant transpiration is sourced from water less than one month old. This strong preference for young water indicates that the LIFO assumption may be fairly accurate. Miguez-Macho and Fan (2021)'s Figure S8 shows the relative fraction of transpiration from recent rain across the continental US. Although their map is not directly comparable to our minimum ET age map in Figure 2, the qualitative similarities are striking: the smallest fraction of recent rain occurs in western states, particularly in upland regions, in a very similar pattern to where we calculated the oldest minimum ET ages. The Miguez-Macho and Fan (2021) approach relies on a state-of-the art hydrological model informed by a large literature compilation of stable isotope studies; the fact that our simple mass balance approach yields similar results is encouraging.

4.3 Uncertainty

Our estimates of flux-weighted ET ages should provide an accurate lower-bound on true ages subject to the accuracy of the precipitation and evapotranspiration flux datasets and to the extent that there are no unaccounted for input fluxes that make younger water available to ET. One such flux, occult precipitation (fog, dew or mist), can constitute a significant plant water source in some ecosystems during dry periods (Limm et al., 2009) and is not typically incorporated into distributed precipitation flux datasets. Our analysis also does not account for lateral influx of saturated zone or surface water (e.g., as groundwater or streamflow originating outside of the pixel) that subsequently becomes evapotranspired. This unaccounted-for input flux is less likely to result in inaccurate lower-bound age estimations, due to the fact that these water fluxes would typically consist of relatively old water, and due to the fact that our pixels are much larger than typical ridge-valley hillslope scales where lateral transport may be most significant. Irrigation, if considered to be 'new' water, would also likely result in incorrect lower bound ET age inferences; we deliberately excluded agricultural and urban areas from our analysis for this reason. Spatial intra-pixel flux heterogeneities could also bias the ET age estimation procedure, and for this reason the evaluation spatial scale should be kept as small as is reasonably possible.

5 Conclusions

Storage selection functions provide a coherent approach for modeling water ages (Rinaldo et al., 2015). However, they have traditionally been parameterized with the aid of tracer data, and little such data exists for ET fluxes at large scales. Here we show how the assumption of a last-in, first-out storage selection function for ET can constrain ET ages from distributed water fluxes alone without the need for tracer data or model parameters. We demonstrated how this storage selection function yields a lower-bound on true ET ages over a time period of record, and applied the simple approach to the continental US. The oldest flux-weighted minimum water ages reach several months and are found in western states, typically in upland areas that experience relatively high asynchronicity between precipitation and energy supply. The resulting dataset can be used as a benchmark to compare against other more complicated age estimation procedures.

Appendix A Demonstration of minimum age

The 'last-in, first-out' (LIFO) algorithm provides a lower bound on the flux-weighted age of ET over some time period of interest. To demonstrate this, we refer to results from an analogous problem in queuing theory. In this problem, customers (precipitation) arrive to a shop (subsurface storage) and must all be served (used for ET). This problem makes a direct analogy if we consider P and ET to consist of infinitesimal, discrete water parcels.

Kingman (1962) demonstrated that any procedure followed for serving the customers will result in the same average wait time (ET age). This means that if there is a set of precipitation that must be used for ET, then the mean age of ET will be the same regardless of how that precipitation is allocated to ET. However, in the case of precipitation and ET, there is generally more precipitation than ET over long timescales, meaning that some precipitation is never used for ET. Thus, in order to minimize the mean ET age a set of precipitation to use for ET must be selected from all available precipitation inputs. The only way to achieve different mean ages is by selecting different sets of precipitation to use.

The LIFO algorithm provides one method for selecting a set of precipitation inputs and assigning them to ET. Any algorithm that selects the same set of precipitation (regardless of how that precipitation is assigned to ET) will result in the same mean ET age. We can test whether LIFO is the algorithm which produces the minimum estimate of flux-weighted ET age by comparing LIFO to another hypothetical algorithm, where we assume that the selected precipitation input set is different from that selected by LIFO. We can call this set A. In order for the hypothetical algorithm to achieve a younger age than LIFO, then there must be a set of P parcels that are different between A and the set chosen by LIFO. However, LIFO by design selects all of the youngest precipitation available, so the set A must have older precipitation if it is different from LIFO.

To see this, assume that there are n parcels different between the set chosen by LIFO and A. We can line up the n parcels from LIFO in chronological order and do the same for the n parcels in A that replace them. Beginning from the youngest end of the set, the parcel chosen by LIFO was the youngest water available in storage given all previous choices. The youngest parcel that could replace it is the youngest parcel in the set of n from A. Any more recently fallen precipitation must (a) already be in the set of P chosen by LIFO, which cannot be the case since this is the set of parcels different between LIFO and A, or (b) is not included in LIFO because it falls too late in the timeseries, meaning that it would not be possible to assign that precipitation to ET since all of the ET following that precipitation already has precipitation parcels to account for it, and this P must be used before it fell, which is also impossible. This means that the parcel from LIFO must be replaced by an older parcel in A. This ordering by chronology can be thought of as a swap, and the preceding argument holds for each swap.

Appendix B Open Research

Complete code for querying the input datasets and reproducing the analysis, and the resulting output georeferenced datasets (provided as a multiband GeoTIFF file) is hosted at the following repository on Hydroshare: `http://www.hydroshare.org/resource/9740fd0142144c8e8bf43876eedec308`

Acknowledgments

Funding was provided by Simon Fraser University, a Natural Sciences and Engineering Research Council of Canada Discovery Grant, the Canadian Foundation for Innovation/British Columbia Knowledge Development Fund, and the USDA Forest Service Pacific Southwest Research Station with funds administered by Oak Ridge Institute for Science and Education (ORISE).

References

Abatzoglou, J. T., Dobrowski, S. Z., Parks, S. A., & Hegewisch, K. C. (2018). Terraclimate, a high-resolution global dataset of monthly climate and climatic water balance from 1958–2015. *Scientific data*, *5*(1), 1–12.

Allen, S. T., Kirchner, J. W., Braun, S., Siegwolf, R. T., & Goldsmith, G. R. (2019). Seasonal origins of soil water used by trees. *Hydrology and Earth System Sciences*, *23*(2), 1199–1210.

Asenjan, M. R., & Danesh-Yazdi, M. (2020). The effect of seasonal variation in precipitation and evapotranspiration on the transient travel time distributions. *Advances in Water Resources*, *142*, 103618.

Bedewy, A. M., Sun, Y., & Shroff, N. B. (2019a). The age of information in multihop networks. *IEEE/ACM Transactions on Networking*, *27*(3), 1248–1257.

Bedewy, A. M., Sun, Y., & Shroff, N. B. (2019b). Minimizing the age of information through queues. *IEEE Transactions on Information Theory*, *65*(8), 5215–5232.

Benettin, P., Nehemy, M. F., Asadollahi, M., Pratt, D., Bensimon, M., McDonnell, J. J., & Rinaldo, A. (2021). Tracing and closing the water balance in a vegetated lysimeter. *Water Resources Research*, *57*(4), e2020WR029049.

Botter, G., Bertuzzo, E., & Rinaldo, A. (2011). Catchment residence and travel time distributions: The master equation. *Geophysical Research Letters*, *38*(11).

Costa, M., Codreanu, M., & Ephremides, A. (2016). On the age of information in status update systems with packet management. *IEEE Transactions on Information Theory*, *62*(4), 1897–1910.

Crockford, R., & Richardson, D. (2000). Partitioning of rainfall into throughfall, stemflow and interception: effect of forest type, ground cover and climate. *Hydrological processes*, *14*(16-17), 2903–2920.

Daly, C., Halbleib, M., Smith, J. I., Gibson, W. P., Doggett, M. K., Taylor, G. H., ... Pasteris, P. P. (2008). Physiographically sensitive mapping of climatological temperature and precipitation across the conterminous united states. *International Journal of Climatology: a Journal of the Royal Meteorological Society*, *28*(15), 2031–2064.

Dralle, D. N., Hahm, W. J., Chadwick, K. D., McCormick, E., & Rempe, D. M. (2021). Accounting for snow in the estimation of root zone water storage capacity from precipitation and evapotranspiration fluxes. *Hydrology and Earth System Sciences*, *25*(5), 2861–2867.

Evaristo, J., Kim, M., van Haren, J., Pangle, L. A., Harman, C. J., Troch, P. A., & McDonnell, J. J. (2019). Characterizing the fluxes and age distribution of soil water, plant water, and deep percolation in a model tropical ecosystem. *Water Resources Research*, *55*(4), 3307–3327.

Feng, X., Thompson, S. E., Woods, R., & Porporato, A. (2019). Quantifying asynchronicity of precipitation and potential evapotranspiration in mediterranean climates. *Geophysical Research Letters*, *46*(24), 14692–14701.

Friedl, M., & Sulla-Menashe, D. (2015). Mcd12q1 modis/terra+ aqua land cover type yearly l3 global 500m sin grid v006 [data set]. *NASA EOSDIS Land Processes DAAC*, *10*.

Gorelick, N. (2021, May). *Runs with Arrays.* Retrieved 2022-03-17, from `https://`

medium.com/google-earth/runs-with-arrays-400de937510a

Gorelick, N., Hancher, M., Dixon, M., Ilyushchenko, S., Thau, D., & Moore, R. (2017). Google earth engine: Planetary-scale geospatial analysis for everyone. *Remote sensing of Environment*, *202*, 18–27.

Hahm, W. J., Dralle, D. N., Sanders, M., Bryk, A. B., Fauria, K. E., Huang, M.-H., ... others (2022). Bedrock vadose zone storage dynamics under extreme drought: consequences for plant water availability, recharge, and runoff. *Water Resources Research*, e2021WR031781.

Hahm, W. J., Rempe, D., Dralle, D., Dawson, T., & Dietrich, W. (2020). Oak transpiration drawn from the weathered bedrock vadose zone in the summer dry season. *Water Resources Research*, *56*(11), e2020WR027419.

Harman, C. (2015). Time-variable transit time distributions and transport: Theory and application to storage-dependent transport of chloride in a watershed. *Water Resources Research*, *51*(1), 1–30.

Harman, C. (2019). Age-ranked storage-discharge relations: A unified description of spatially lumped flow and water age in hydrologic systems. *Water Resources Research*, *55*(8), 7143–7165.

Hrachowitz, M., Savenije, H., Bogaard, T., Tetzlaff, D., & Soulsby, C. (2013). What can flux tracking teach us about water age distribution patterns and their temporal dynamics? *Hydrology and Earth System Sciences*, *17*(2), 533–564.

Kaul, S. K., Yates, R. D., & Gruteser, M. (2012). Status updates through queues. In *2012 46th annual conference on information sciences and systems (ciss)* (pp. 1–6).

Kellndorfer, J., Walker, W., Kirsch, K., Fiske, G., Bishop, J., LaPoint, L., ... Westfall, J. (2013). Nacp aboveground biomass and carbon baseline data, v. 2 (nbcd 2000), usa, 2000. *ORNL DAAC*.

Kelly, A. E., & Goulden, M. L. (2016). A montane mediterranean climate supports year-round photosynthesis and high forest biomass. *Tree Physiology*, *36*(4), 459–468.

Kingman, J. F. (1962). The effect of queue discipline on waiting time variance. In *Mathematical proceedings of the cambridge philosophical society* (Vol. 58, pp. 163–164).

Kirchner, J. W., & Allen, S. T. (2020). Seasonal partitioning of precipitation between streamflow and evapotranspiration, inferred from end-member splitting analysis. *Hydrology and Earth System Sciences*, *24*(1), 17–39. Retrieved from https://hess.copernicus.org/articles/24/17/2020/ doi: 10.5194/hess-24-17-2020

Kleinrock, L. (1975). *Queueing Systems* (Vol. I: Theory). Wiley Interscience.

Kuppel, S., Tetzlaff, D., Maneta, M. P., & Soulsby, C. (2020). Critical zone storage controls on the water ages of ecohydrological outputs. *Geophysical Research Letters*, *47*(16), e2020GL088897.

Lapides, D. A., Hahm, W. J., Rempe, D. M., Dietrich, W. E., & Dralle, D. N. (2022). Controls on stream water age in a saturation overland flow-dominated catchment. *Water Resources Research*, *58*(4), e2021WR031665. Retrieved from https://agupubs.onlinelibrary.wiley.com/doi/abs/10.1029/2021WR031665 (e2021WR031665 2021WR031665) doi: https://doi.org/10.1029/2021WR031665

Li, L., Maher, K., Navarre-Sitchler, A., Druhan, J., Meile, C., Lawrence, C., ... others (2017). Expanding the role of reactive transport models in critical zone processes. *Earth-science reviews*, *165*, 280–301.

Limm, E. B., Simonin, K. A., Bothman, A. G., & Dawson, T. E. (2009). Foliar water uptake: a common water acquisition strategy for plants of the redwood forest. *Oecologia*, *161*(3), 449–459.

Maher, K. (2010). The dependence of chemical weathering rates on fluid residence time. *Earth and Planetary Science Letters*, *294*(1-2), 101–110.

Maxwell, R. M., Condon, L. E., Danesh-Yazdi, M., & Bearup, L. A. (2019). Exploring source water mixing and transient residence time distributions of outflow and evapotranspiration with an integrated hydrologic model and lagrangian particle tracking approach. *Ecohydrology*, *12*(1), e2042.

McCormick, E. L., Dralle, D. N., Hahm, W. J., Tune, A. K., Schmidt, L. M., Chadwick, K. D., & Rempe, D. M. (2021). Widespread woody plant use of water stored in bedrock. *Nature*, *597*(7875), 225–229.

McGuire, K. J., & McDonnell, J. J. (2006). A review and evaluation of catchment transit time modeling. *Journal of Hydrology*, *330*(3-4), 543–563.

Meinzer, F. C., Brooks, J., Domec, J.-C., Gartner, B. L., Warren, J., Woodruff, D., ... Shaw, D. (2006). Dynamics of water transport and storage in conifers studied with deuterium and heat tracing techniques. *Plant, cell & environment*, *29*(1), 105–114.

Miguez-Macho, G., & Fan, Y. (2021). Spatiotemporal origin of soil water taken up by vegetation. *Nature*, *598*(7882), 624–628.

Oki, T., & Kanae, S. (2006). Global hydrological cycles and world water resources. *science*, *313*(5790), 1068–1072.

Pedrazas, M. A., Hahm, W. J., Dralle, D., Nelson, M. D., Breunig, R. E., Fauria, K. E., ... others (2021). The relationship between topography, bedrock weathering, and water storage across a sequence of ridges and valleys. *Journal of Geophysical Research: Earth Surface. 126 (4): 217*, *126*(4).

Peel, M. C., Finlayson, B. L., & McMahon, T. A. (2007). Updated world map of the köppen-geiger climate classification. *Hydrology and earth system sciences*, *11*(5), 1633–1644.

PRISM Climate Group. (2021). *PRISM Climate Data* (Tech. Rep.). Oregon State University. Retrieved from `http://prism.oregonstate.edu` (00000)

Rempe, D. M., McCormick, E. L., Hahm, W. J., Persad, G. G., Cummins, C., Lapides, D. A., ... Dralle, D. N. (pre-print). Resilience of woody ecosystems to precipitation variability. *EarthArxiv*. doi: https://doi.org/10.31223/X5XW7D

Rinaldo, A., Benettin, P., Harman, C. J., Hrachowitz, M., McGuire, K. J., Van Der Velde, Y., ... Botter, G. (2015). Storage selection functions: A coherent framework for quantifying how catchments store and release water and solutes. *Water Resources Research*, *51*(6), 4840–4847.

Schlesinger, W. H., & Jasechko, S. (2014). Transpiration in the global water cycle. *Agricultural and Forest Meteorology*, *189*, 115–117.

Seeger, S., & Weiler, M. (2021). Temporal dynamics of tree xylem water isotopes: in situ monitoring and modeling. *Biogeosciences*, *18*(15), 4603–4627.

Smith, A., Tetzlaff, D., Kleine, L., Maneta, M., & Soulsby, C. (2021). Quantifying the effects of land use and model scale on water partitioning and water ages using tracer-aided ecohydrological models. *Hydrology and Earth System Sciences*, *25*(4), 2239–2259.

Soulsby, C., Birkel, C., Tetzlaff, D., et al. (2016). Characterizing the age distribution of catchment evaporative losses. *Hydrological Processes*, *30*(8), 1308–1312.

Sprenger, M., Stumpp, C., Weiler, M., Aeschbach, W., Allen, S. T., Benettin, P., ... others (2019). The demographics of water: A review of water ages in the critical zone. *Reviews of Geophysics*, *57*(3), 800–834.

Tripathi, V., Talak, R., & Modiano, E. (2019). Age of information for discrete time queues. *arXiv preprint arXiv:1901.10463*.

Visser, A., Thaw, M., Deinhart, A., Bibby, R., Safeeq, M., Conklin, M., ... Van der Velde, Y. (2019). Cosmogenic isotopes unravel the hydrochronology and water storage dynamics of the southern sierra critical zone. *Water Resources Research*, *55*(2), 1429–1450.

Wang-Erlandsson, L., Bastiaanssen, W. G., Gao, H., Jägermeyr, J., Senay, G. B., Van Dijk, A. I., ... Savenije, H. H. (2016). Global root zone storage capacity from satellite-based evaporation. *Hydrology and Earth System Sciences*, *20*(4), 1459–1481.

Wilusz, D., Harman, C., Ball, W., Maxwell, R., & Buda, A. (2020). Using particle tracking to understand flow paths, age distributions, and the paradoxical origins of the inverse storage effect in an experimental catchment. *Water Resources Research*, *56*(4), e2019WR025140.

Xu, J., & Gautam, N. (2020). Peak age of information in priority queuing systems. *IEEE Transactions on Information Theory*, *67*(1), 373–390.

Zhang, Y., Kong, D., Gan, R., Chiew, F. H., McVicar, T. R., Zhang, Q., & Yang, Y. (2019). Coupled estimation of 500 m and 8-day resolution global evapotranspiration and gross primary production in 2002–2017. *Remote sensing of environment*, *222*, 165–182.